Progress in Organic Coatings 76 (2013) 944–949

Contents lists available at SciVerse ScienceDirect

Progress in Organic Coatings

journal homepage: www.elsevier.com/locate/porgcoat

Investigation of PSt-MWCNT concentration on epoxyacrylate photopolymerization and conductivity of polymer films

Zekeriya Doğruyol[a], Gokhan Temel[b], Sevnur K. Doğruyol[c], Önder Pekcan[d], Nergis Arsu[c,*]

[a] Istanbul University, Department of Engineering Science, 34850 Istanbul, Turkey
[b] Yalova University, Department of Polymer Engineering, 77100 Yalova, Turkey
[c] Yildiz Technical University, Chemistry Department, 34320 Istanbul, Turkey
[d] Faculty of Arts and Science, Kadir Has University, 34320 Istanbul, Turkey

ARTICLE INFO

Article history:
Received 15 July 2012
Accepted 20 August 2012
Available online 21 November 2012

Keywords:
Modified PSt-MWCNT
Nanocomposite
Photopolymerization kinetics
Filter effect

ABSTRACT

Photopolymerization kinetics and conductivity changes of epoxyacrylate composites for various loading modified PSt-MWCNT weight fractions changing from 0.0025 to 0.2 wt.% were evaluated by performing photo differential scanning calorimetry (photo-DSC) and four point conductivity measurements. 0.2% PSt-MWCNT additive polymeric films had their electrical conductivity boosted by 6% more than non-additive polymeric films.

1. Introduction

Polymer nanocomposites with carbon nanotube fillers have generated much interest among researchers for the improvement of their mechanical properties and electrical conductivity [1–8]. In recent years, CNT composites have been a major area of research and development, where they are used as reinforcing particles embedded in a matrix (polymeric, ceramic or metallic) to confer the CNTs' inherent properties to the composites which then gain enhanced functionalities. They are excellent nano-filler materials for transforming electrically non-conducting polymers into conductive materials, which have shown potential applications in electromagnetic interference (EMI) shielding, photovoltaic devices, and transparent conductive coatings [9–17].

Although CNTs exhibit excellent properties, such as low mass density, electrical conductivity and, mechanically, as a nanocomposite component, they suffer from self-aggregation and poor solubility in organic solvents and water arising from their rigid honeycomb structures [18]. In order to overcome the latter drawback, several approaches involving non-covalent and covalent functionalization methods were reported and CNTs with improved solubility were obtained. Non-covalent functionalizations such as π–π stacking interactions between the surface of CNTs and polynuclear groups of polymers were based on Van der Waals forces [19]. Covalent functionalization examples include grafting of macromolecules using both "grafting onto" [20–22] and "grafting from" [23] approaches. The "grafting onto" method is the most widely used functionalization approach to prepare modified CNTs with various types of polymers. Depending on the type of polymer used, the resultant composites may exhibit hydrophilic [24], hydrophobic [25] or amphiphilic [26] properties.

In photopolymerization experiments, mainly type I (by bond cleavage) and type II (by H-abstraction) initiators are employed [27]. Although type I photoinitiators are more effective than type II initiators, type II initiators operating in the visible range are advantageous in terms of energy policies. Recently, mercapto derivatives [28], carboxylic acid derivatives [29,30], anthracene derivatives [31,32] and morpholine-attached [33] TX initiators were used for the polymerization of acrylates and methacrylates as type II one-component photoinitiators. Another approach was also undertaken and thioxanthone-benzotriazole was synthesized, which presented stabilizer and initiator properties in one-component initiators [34].

In previous studies we conducted, the efficiency of 2-mercaptothioxanthone (TX-SH) was investigated [28]. A thiol derivative of thioxanthone TX-SH photoinitiator serves as both a triplet photo-sensitizer [35] and a hydrogen donor for free radical polymerization. The mechanism of photoinitiation is based on the intermolecular reaction of the triplet, ^{3}TX-SH*, with the thiol moiety of ground state TX-SH. The resulting thyl radical initiates polymerization (Scheme 1) [28].

We report here the results, by means of photopolymerization kinetics and the conductivity of polymeric films, of adding of

* Corresponding author.
E-mail addresses: dogruyolz@gmail.com, arsunergis@gmail.com (N. Arsu).

0300-9440/$ – see front matter © 2012 Elsevier B.V. All rights reserved.
http://dx.doi.org/10.1016/j.porgcoat.2012.10.013

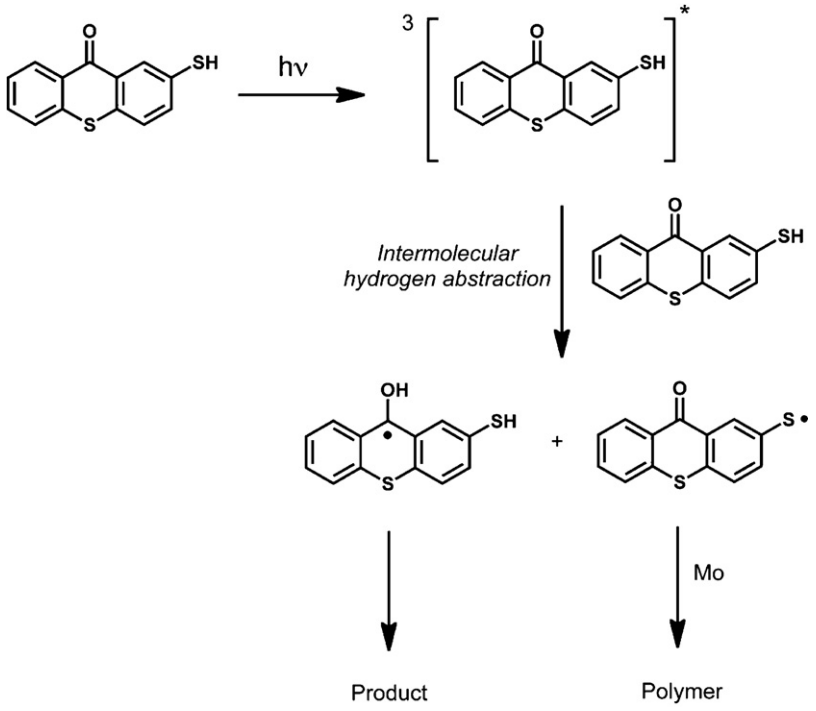

Scheme 1. Photoinitiation mechanism of TX-SH.

polystyrene grafted multiwall carbon nanotube MWCNT by thiol-ene click chemistry via the thermal initiation method.

2. Experimental

2.1. Materials

2-Mercaptothioxanthone (TX-SH) was synthesized according to the previously described procedure [28]. Dimethylformamide (DMF, 99+%, Aldrich) was distilled over CaH_2 under reduced pressure. Epoxy diacrylate (EA) and tripropyleneglycoldiacrylate (TPGDA) were obtained from Cognis France. Styrene (St, 99%, Aldrich) was distilled under reduced pressure before use. 2,2′-Azobis(isobutyronitrile) (AIBN, 98%, Aldrich) was recrystallized from ethanol. Tetrahydrofuran (THF, 99.8%, J.T. Baker) was dried and distilled over benzophenone-Na. *N*,*N*,*N*′,*N*″,*N*″-Pentamethyldiethylenetriamine (PMDETA, Aldrich) was distilled over NaOH ethyl-2-bromopropionate (>99%, Aldrich) and trimethylolpropane tris(2-mercaptoacetate) (technical grade, Aldrich) was used as received. Multiwall carbon nanotube (MWCNT) Baytubes® C 150 P (Bayer) and all other reagents were used as received.

2.2. Preparation of formulations

Photoinitiator (TX-SH) concentration was held constant (0.5%, w/w) for all formulations; DMF was used to dissolve the initiator easily and various weight percentages of PSt-MWCNT (0:0.0025:0.0050:0.010:0.0250:0.0500:0.1000:0.2000 (%, w/w)) content in $CHCl_3$ and epoxydiacrylate (80%) and tripropylenegylcoldiacrylate (20%) were added and the formulations were sonicated and then stirred for one day at 500 rpm.

2.2.1. General procedure for atom transfer radical polymerization

To a Schlenk tube equipped with a magnetic stirring bar, the degassed monomer (St, 44 mmol), ligand (PMDETA, 0.44 mmol), catalyst (CuBr, 0.44 mmol) and initiator (ethyl-2-bromopropionate, 0.44 mmol) were added, respectively. The tube was degassed by three freeze-pump-thaw cycles, left under vacuum, and placed in a 90 °C thermostated oil bath. After polymerization, the reaction mixture was diluted with THF and then passed through a column of neutral alumina to remove the metal salt. The excess of THF and unreacted monomer were evaporated under reduced pressure. The polymer was dissolved in THF and precipitated in 10-fold excess methanol. The resulting polymer was dried in a vacuum oven at room temperature. Molecular weights and molecular weight distributions of the polymers (M_n = 3000 g mol^{-1}, PDI = 1.18) were determined by GPC.

2.2.2. Synthesis of thiol end-functional polystyrene (PSt-SH)

The thiol end-functional polystyrenes were synthesized from the above obtained PSt-Br by organic substitution reaction following the literature procedure [36]. Thus, a mixture of 1.0 g of polystyrene (PSt-Br), of thiourea (0.08 g, 1.05 mmol, 10 equiv.) and 30 ml of DMF was heated at 100 °C under flow for 24 h. NaOH (0.042 g, 1.05 mmol, 10 equiv.) which was dissolved in 0.8 ml of water, was added and the mixture heated to 110 °C for 24 h. Two drops of 95% sulfuric acid in 0.5 ml of water were added and the

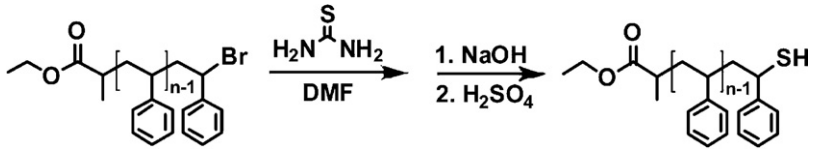

Scheme 2. Overall process for the synthesis of thiol end functional polystyrene.

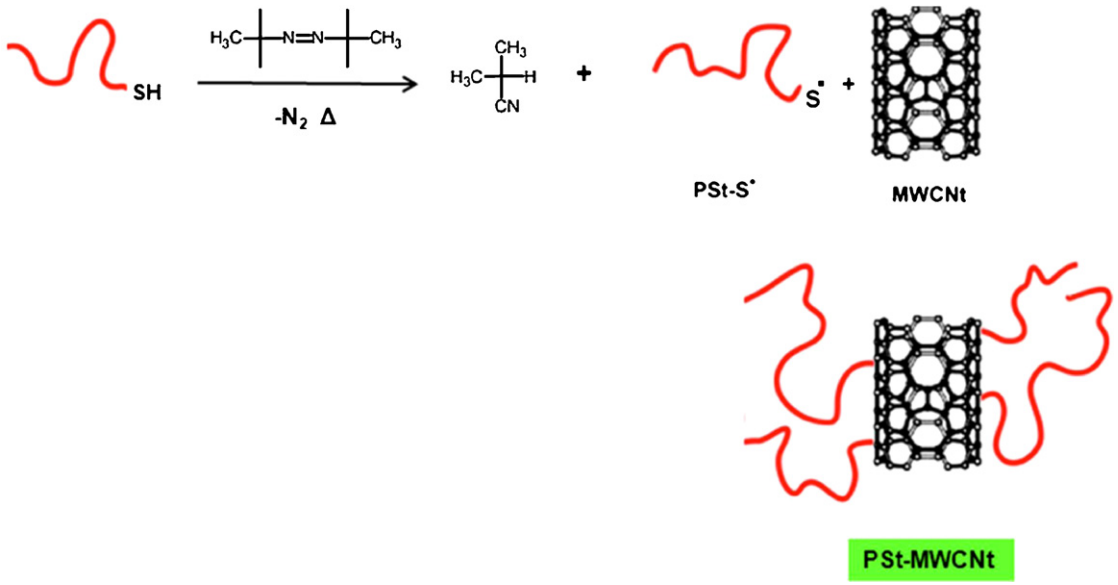

Scheme 3. Modification of MWCNT with thiol-ene click chemistry with PSt-SH.

mixture was stirred at room temperature for an additional 5 h. The functionalized polymer was purified by successive precipitations in methanol (Scheme 2).

^{1}H NMR ($CDCl_3$, 250 MHz): δ = 7.25–6.24 (m, aromatic protons of PS), 3.94 (broad, 2 H, —CH_2—O—C=O), 3.51 ppm (broad, 1 H, —CH—S).

2.2.3. Modification of MWCNT with PSt-SH by thiol-ene click chemistry

PSt-SH (150 mg) and a catalytic amount of AIBN (1–2%, w/w) were dissolved in 30 ml of DMF, and 50 mg MWCNT was added. The mixture was sonicated for 10 min in an ultrasonic bath and the resulting suspension was bubbled with argon for 15 min. Then the suspension was sonicated again for 10 min and allowed to stir at 80 °C overnight. At the end of the period, the resulting mixture was centrifuged to remove solvent and unreacted polymer. Modified MWCNT was redispersed in fresh THF using mild sonication and then centrifuged again. The redispersion and recentrifugation process was then repeated three times to remove any free PSt. The final product was dried in vacuum.

^{1}H NMR ($CDCl_3$, 250 MHz): δ = 7.38–6.25 (m, aromatic protons of PS), 2.34–1.22 (m, aliphatic protons of PS) (Scheme 3).

2.3. Photo differential scanning calorimeter (photo-DSC)

The heat of the photoinitiated polymerization reaction was measured by means of a photo differential scanning calorimeter. The photoinitiated polymerization of EA/TPGDA with various concentrations of PSt-MWCNT in the presence of TX-SH (0.5 wt.%) was performed in a photo-DSC setup (TA-DSCQ100). UV light was applied from a medium pressure mercury lamp at a constant intensity of 40 mW/cm^2 for 3 min under a nitrogen flow of 50 ml/min at room temperature (isothermal mode). The weight of the samples 2 ± 0.1 mg was placed into an open aluminum liquid DSC pan. Measurements were carried out under identical conditions and recorded at a sampling interval of 0.05 s/point. The thickness of cured thin films was about 0.25 mm according to the previously described procedure [37].

The reaction heat liberated in the polymerization is directly proportional to the number of acrylates reacted in the system. By integrating the area under the exothermic peak, the conversion of the acrylate groups (C) or the extent of the reaction was determined according to Eq. (1):

$$C = \frac{\Delta H_t}{\Delta H_0^{\text{theory}}} \quad (1)$$

where ΔH_t is the reaction heat evolved at time t and $\Delta H_0^{\text{theory}}$ is the theoretical heat for complete conversion. A reaction heat for an acrylate double bond polymerization of $\Delta H_0^{\text{theory}} = 86.25$ kJ/mol was used [38,39]. The rate of polymerization (R_p) is directly related to the heat flow (dH/dt) as in Eq. (2):

$$R_p = \frac{dC}{dt} = \frac{(dH/dt)}{\Delta H_0^{\text{theory}}} \quad (2)$$

Electrical resistivity measurement

The electrical resistivities of the films were conducted with the Signatone system, incorporated with a four-point cylindrical probe. The four-point probe has four probes in a straight line with an equal inter-probe spacing of 1.56 mm. The probe needle radius is 100 μm. The electrical resistance of the films, Rs, can be obtained from Eq. (3)

$$\text{Rs} = 4.53 \times \frac{V}{I} \quad (3)$$

where I is the constant current that passed through the two outer probes and V is the output voltage measured across the inner probes with the Keithley 2400 source-meter.

3. Results and discussion

3.1. Kinetic assessment of photopolymerization

The photocuring of epoxydiacrylate (80%) diluted with TPGDA (20%) in the presence of TX-SH photoinitiator with various PSt-MWCNT loading was followed by photo-DSC. To study the photopolymerization kinetics of nanocomposites by photo-DSC is important and provides heat flow data. The heat flow can be converted by Eq. (3) to the ultimate percentage conversion and the polymerization rate for a given amount of formulation is given in Table 1. However, it should be pointed out that although the solubility of MWCNT is significantly increased by the modification, there still exist some dispersion problems which interfere with the light

Table 1
Surface resistance and electrical conductivities of photopolymerized films containing different concentrations of PSt-MWCNT.

[PSt-MWCNT] (%)	$10^9 \times \rho_s(\Omega)$	$10^{-9} \times \sigma$ (Siemens)
0.0000	1.746	0.573
0.0025	1.743	0.574
0.0050	1.741	0.574
0.0100	1.736	0.576
0.0500	1.732	0.577
0.1000	1.708	0.585
0.2000	1.639	0.610

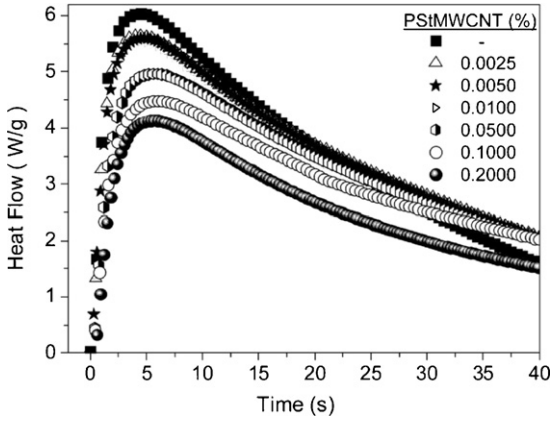

Fig. 1. Heat flow versus time curves of EA/TPGDA monomer, photoinitiated with TX-SH, which contains various amounts of PSt-MWCNT.

transmission, especially for the highest loadings of PSt-MWCNTs. The profiles of the photopolymerization of EA + TPGDA with various PSt-MWCNT loadings initiated by TX-SH are shown in Figs. 1–3 at 25 °C by UV light with an intensity of 40 mW/cm^2.

Adding between a range of 0.0025% and 0.2% PSt-MWCNT to the UV-curable formulations gradually led to lower polymerization rates of up to 0.5% loading of PSt-MWCNT. With 0.2% of PSt-MWCNT loading, the conversion percentage decreased at least 20% compared to formulations which had no PSt-MWCNT. The correlation between various loading amounts of PSt-MWCNT and the maximum of rate of polymerization and final conversion percentages are summarized in Figs. 4 and 5. Increasing the amount of PSt-MWCNT reduces the light penetration and in addition, the probability of producing of initiating thiyl radicals from TX-SH is lowered, which is reflected in both the R_p and final conversion C_s values.

Formulations, which are used for photo-DSC experiments, have been coated with the doctor blade method in order to examine the

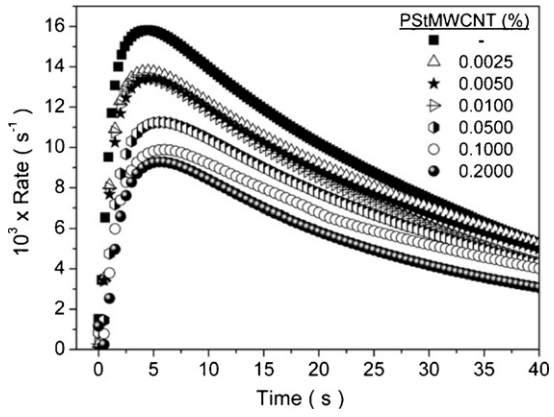

Fig. 2. Rate of polymerization versus time curves of EA/TPGDA monomer, photoinitiated with TX-SH, which contains various amounts of PSt-MWCNT.

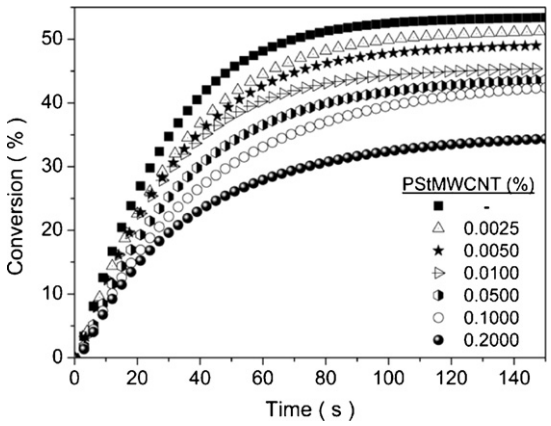

Fig. 3. Monomer conversion percentages versus time curves of EA/TPGDA monomer, photoinitiated with TX-SH, which contains various amounts of PSt-MWCNT.

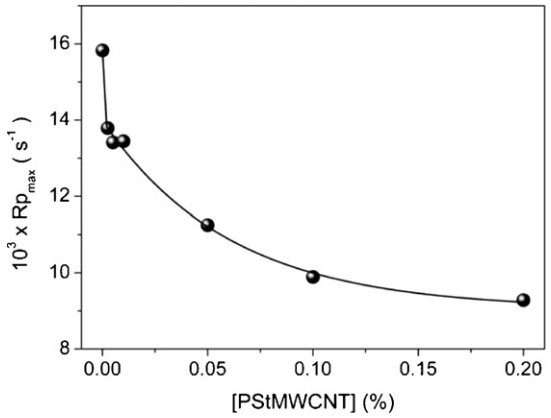

Fig. 4. PSt-MWCNT concentration versus the rate of polymerization ($R_{p_{max}}$) of EA/TPGDA monomer, photoinitiated with TX-SH.

UV light penetration onto the films. These formulations were placed into 1 cm × 1 cm glasses and cured with 8 passes under a Mini-UV-cure unit. The polymeric films obtained, consisting of the various concentration of PSt-MWCNT, are given in Fig. 6.

To demonstrate the cut-off light penetration of formulations containing various amounts of PSt-MWCNT, transmission spectra of all UV cured films were taken and are given in Fig. 7.

The TX-SH photoinitiator has an absorption maximum at 382 nm and as seen from Fig. 7, increasing the amount of

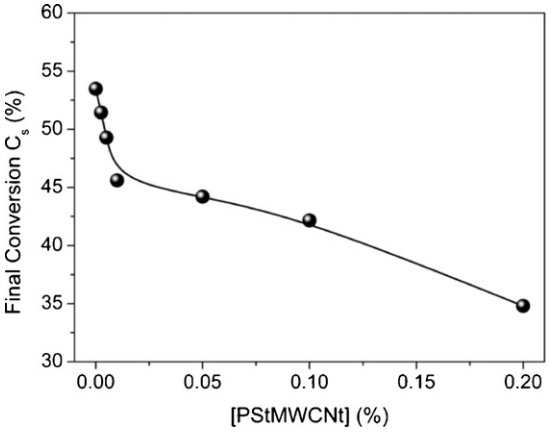

Fig. 5. PSt-MWCNT concentrations versus change of final conversion (C_s) of EA/TPGDA monomer, photoinitiated with TX-SH.

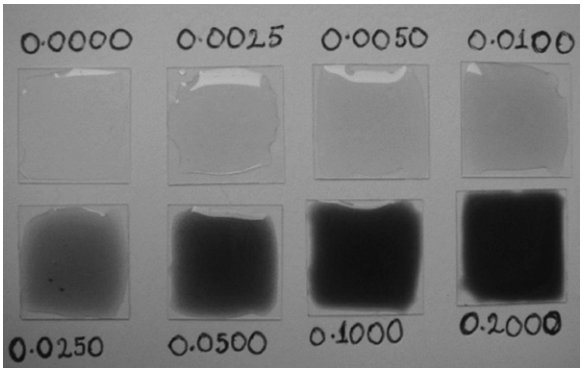

Fig. 6. The pictures of UV cured polymeric films consisting of different concentrations of PSt-MWCNT.

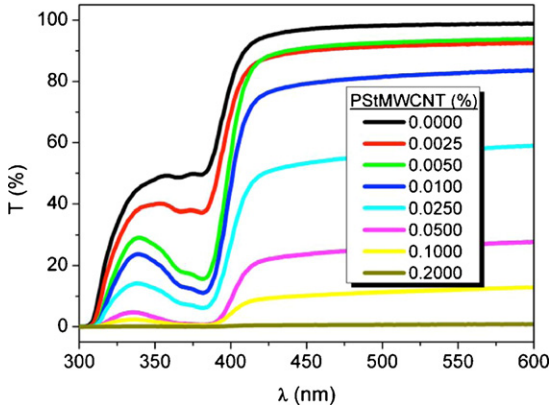

Fig. 7. UV–vis region transparency spectra of UV cured thin films that contain. PSt-MWCNT in different concentrations.

PSt-MWCNT decreases the transmission percentage of cured films and this diminishes the effect of the photoinitiator's light absorption capability. This effect is summarized in Fig. 8.

Examining conductivity properties of epoxyacrylate based films containing various amounts of PSt-MWCNT

Fig. 9 shows the morphology of PSt-MWCNT containing photocured nanocomposite films. The figures show no obvious agglomeration of PSt-MWCNT in the matrix and indicate good interaction between filler and polymer matrix. The good dispersion

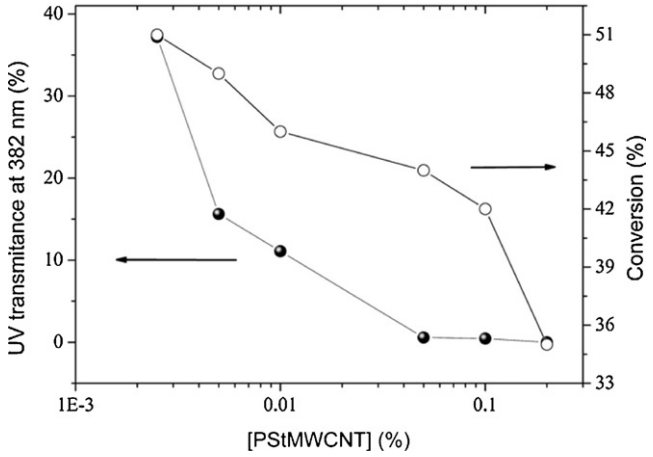

Fig. 8. Permeability intensities and monomer conversation percentages of epoxyacrylate films at 382 nm, which contain different concentrations of PSt-MWCNT.

of PSt-MWCNT within the polymer matrix helps to enhancement of the physical properties of nanocomposite coating.

TX-SH photoinitiator, EA + TPGDA monomer and PSt-MWCNT at different concentrations were coated onto coverglass and then cured by passing through a Mini UV-cure unit. The conductivity of the obtained film's surface was measured by using a four-point probe. With this method, surface resistance values were obtained using two outer electrodes and two inner electrodes. A current was sent from the two outer electrodes to the two inner electrodes and then the current between the two inner electrodes was measured. By calculating the reverse of the resistance values, conductivities were determined. These procedures were conducted for thin films containing different concentrations of PSt-MWCNT and the DC conductivity values dependent on logarithmic concentration can be observed in Fig. 10. All surface resistivity and conductivity values have been summarized in Table 1.

Table 1 shows surface resistance and electrical conductivities of epoxyacyrylate based films, photo-cured with TX-SH, containing different concentrations of PSt-MWCNT. In comparison, 0.2% PSt-MWCNT additive polymeric films had a 6% boost of electrical conductivity compared with non-additive polymeric films.

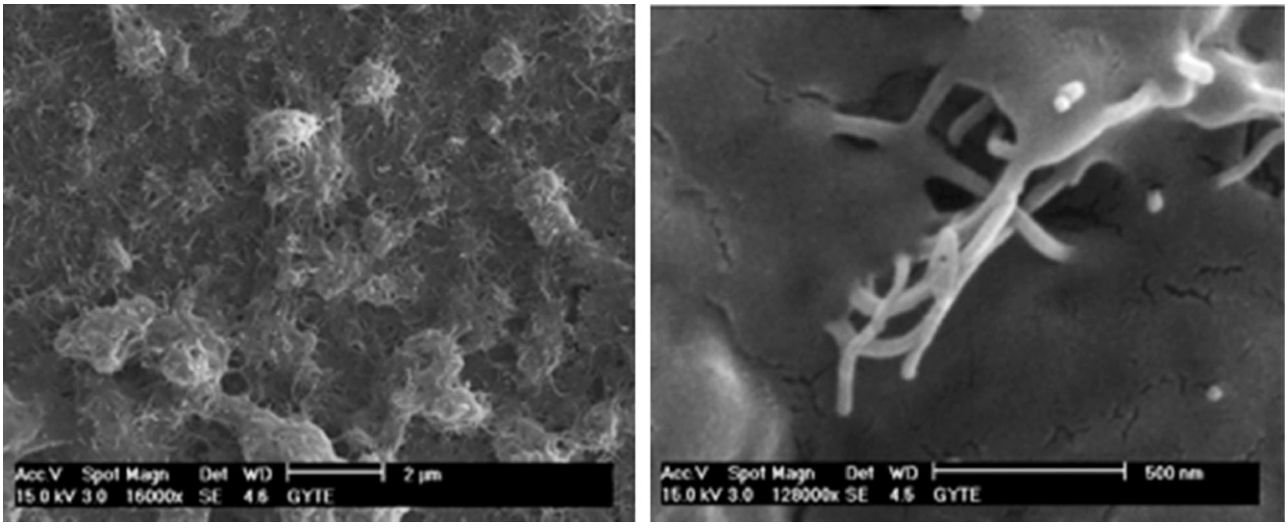

Fig. 9. SEM images of epoxyacrylate film which contains PSt-MWCNT (0.2%).

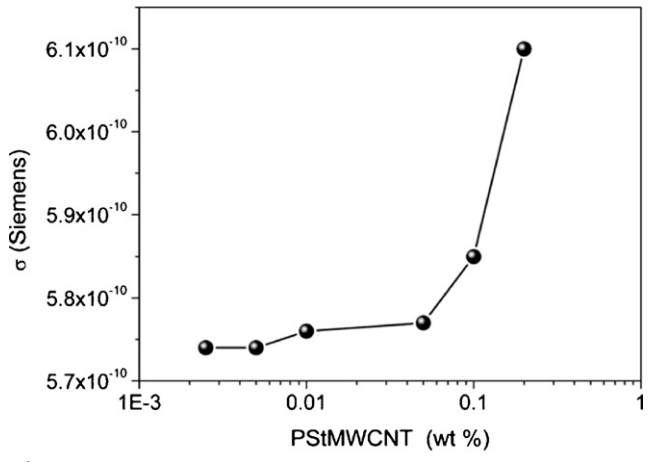

Fig. 10. DC conductivity values of polymeric films dependent on PSt-MWCNT concentration using point method.

4. Conclusion

In this work, thiol functional polystyrene was successfully attached to the MWCNT with thermal initiated thiol-ene click strategy. Different concentrations of resulting PSt-MWCNT were used as filler in diacrylates formulations and conductivity of the polymeric films were found to be $0.610 \times 10^{-9} \times \sigma$ (Siemens) in maximum loading of the PSt-MWCNT (0.2%). Meanwhile, increase of the PSt-MWCNT loading is inversely proportional to penetration of the light into the cured films and this negatively affects the light absorption behavior of photoinitiator during the photoinduced free radical polymerization.

References

[1] W. Bauhofer, J.Z. Kovacs, Compos. Sci. Technol. 69 (2009) 1486–1498.
[2] (a) Z. Ounaies, C. Park, K.E. Wise, E.J. Siochi, J.S. Harrison, Compos. Sci. Technol. 63 (2003) 1637–1646;
(b) E. Kymakis, G.A.J. Amaratunga, J. Appl. Phys. 99 (2006) 084302.
[3] E.B. Kilbride, J.N. Coleman, J. Fraysse, P. Fournet, M. Cadek, M.A. Drury, S. Hutzler, S. Roth, W.J. Blau, J. Appl. Phys. 92 (2002) 4024–4030.
[4] C.A. Martin, J.K.W. Sandler, M.S.P. Shaffer, M.K. Schwarz, W. Bauhofer, K. Schulte, A.H. Windle, Compos. Sci. Technol. 64 (2004) 2309–2316.
[5] J. Sandler, M.S.P. Shaffer, T. Prasse, W. Bauhofer, K. Schulte, A.H. Windle, Polymer 40 (1999) 5967–5971.
[6] J.K.W. Sandler, J.E. Kirk, I.A. Kinloch, M.S.P. Shaffer, A.H. Windle, Polymer 44 (2003) 5893–5899.
[7] N. Hu, Z. Masuda, C. Yan, G. Yamamoto, H. Fukunaga, T. Hashida, Nanotechnology 19 (2008) 215701.
[8] Z. Spitalskya, D. Tasis, K. Papagelis, C. Galiotis, Prog. Polym. Sci. 35 (2010) 340–357.
[9] I.C. Finegan, G.G. Tibbetts, J.M. Ting, M.L. Lake, J. Mater. Sci. 38 (2003) 3485–3490.
[10] H.M. Kim, K. Kim, C.Y. Lee, J. Joo, S. Cho, H.S. Yoon, et al., Appl. Phys. Lett. 84 (2004) 589–591.
[11] H. Ago, K. Petritsch, A.H. Windle, R.H. Friend, Adv. Mater. 11 (1999) 1281–1285.
[12] E. Kymakis, G.A.J. Amaratunga, Appl. Phys. Lett. 80 (2002) 112–114.
[13] G.G. Tibbetts, I.C. Finegan, C. Kwag, Mol. Cryst. Liq. Cryst. 387 (2002) 129–133.
[14] Y. Yang, M.C. Gupta, K.L. Dudley, R.W. Lawrence, Adv. Mater. 17 (2005) 1999–2003.
[15] S.Y. Yang, K. Lozano, H.D. Foltz, R. Jones, Composites A 36 (2005) 691–697.
[16] F.H. Gojny, M.G.H. Wichmann, B. Fiedler, W. Bauhofer, K. Schulte, Composites A 36 (2005) 1525–1535.
[17] M. Ioniță, A. Prună, Prog. Org. Coat. 72 (2011) 647–652.
[18] A. Chiolerio, S. Musso, M. Sangermano, M. Giorcelli, S. Bianco, M. Coisson, A. Priola, P. Allia, A. Taghaferro, Diam. Relat. Mater. 17 (2008) 1590–1595.
[19] Y.H. Yan, J.A. Cui, P. Potschke, B. Voit, Carbon 48 (2010) 2603–2612.
[20] P. Liu, Eur. Polym. J. 41 (2005) 2693–2703.
[21] S.H. Qin, D.Q. Qin, W.T. Ford, D.E. Resasco, J.E. Herrera, Macromolecules 37 (2004) 752–757.
[22] M.S.P. Shaffer, K. Koziol, Chem. Commun. 18 (2002) 2074–2075.
[23] H. Kong, C. Gao, D.Y. Yan, J. Am. Chem. Soc. 126 (2004) 412–413.
[24] W.F. Chen, J.S. Wu, P.L. Kuo, Chem. Mater. 20 (2008) 5756–5767.
[25] S. Akbar, E. Beyou, P. Cassagnau, P. Chaumont, G. Farzi, Polymer 50 (2009) 2535–2543.
[26] Y. Zhang, H.K. He, C. Gao, Macromolecules 41 (2008) 9581–9594.
[27] S. Keskin, N. Arsu, Polym. Bull. 57 (2006) 643–650.
[28] L. Cokbaglan, N. Arsu, Y. Yagci, S. Jockusch, N.J. Turro, Macromolecules 36 (2003) 2649–2653.
[29] M. Aydin, N. Arsu, Y. Yagci, Macromol. Rapid Commun. 24 (2003) 718–723.
[30] M. Aydin, N. Arsu, Y. Yagci, S. Jockusch, N.J. Turro, Macromolecules 38 (2005) 4133–4138.
[31] D.K. Balta, N. Arsu, Y. Yagci, S. Jockusch, N.J. Turro, Macromolecules 40 (2007) 4138–4141.
[32] D.K. Balta, G. Temel, G. Goksu, N. Ocal, N. Arsu, Macromolecules 45 (2012) 119–125.
[33] S.K. Dogruyol, Z. Dogruyol, N. Arsu, J. Polym. Sci. Part A: Polym. Chem. 19 (2011) 4037–4043.
[34] D. Sevinc, F. Karasu, N. Arsu, J. Photochem. Photobiol. A: Chem. 203 (2009) 81–84.
[35] S. Keskin, S. Jockusch, N.J. Turro, N. Arsu, Macromolecules 41 (2008) 4631–4634.
[36] L. Garamszegi, C. Donzel, G. Carrot, T.Q. Nguyen, J. Hilborn, React. Funct. Polym. 55 (2003) 179–183.
[37] Z. Doğruyol, N. Arsu, S. Keskin Doğruyol, Ö. Pekcan, Prog. Org. Coat. 72 (2011) 763–768.
[38] E. Andrzejewska, M. Andrzejewski, J. Polym. Sci. Part A: Polym. Chem. 36 (1998) 665–673.
[39] Z. Doğruyol, N. Arsu, S. Keskin Doğruyol, Ö. Pekcan, Prog. Org. Coat. 74 (2012) 181–185.